

Supporting Information

Large-scale synthesis of porous carbon via one-step CuCl₂ activation of rape pollen for high-performance supercapacitor

Simin Liu, Yeru Liang, Wan Zhou, Wenqiang Hu, Hanwu Dong, Mingtao Zheng,
Hang Hu, Bingfu Lei, Yong Xiao*, Yingliang Liu*

College of Materials and Energy, South China Agricultural University, Guangzhou 510642, China

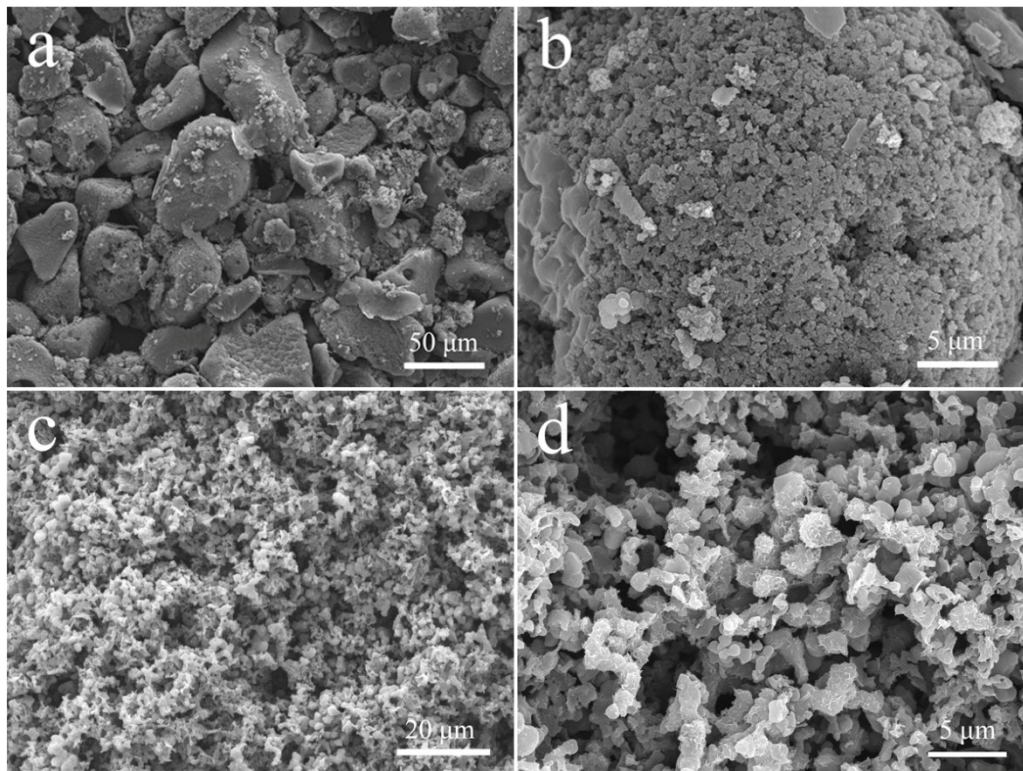


Figure S1. Different magnification SEM images (a, b) of Z-RPC. Different magnification SEM images (c, d) of K-RPC

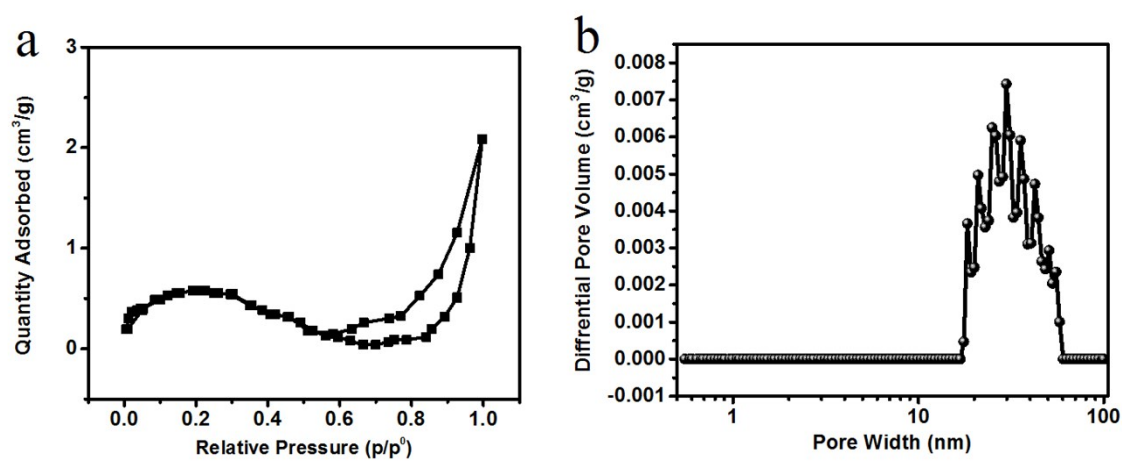


Figure S2. (a) N₂ adsorption-desorption curves of the Blank sample. (b) pore-size distribution (PSD) curves of the Blank sample.

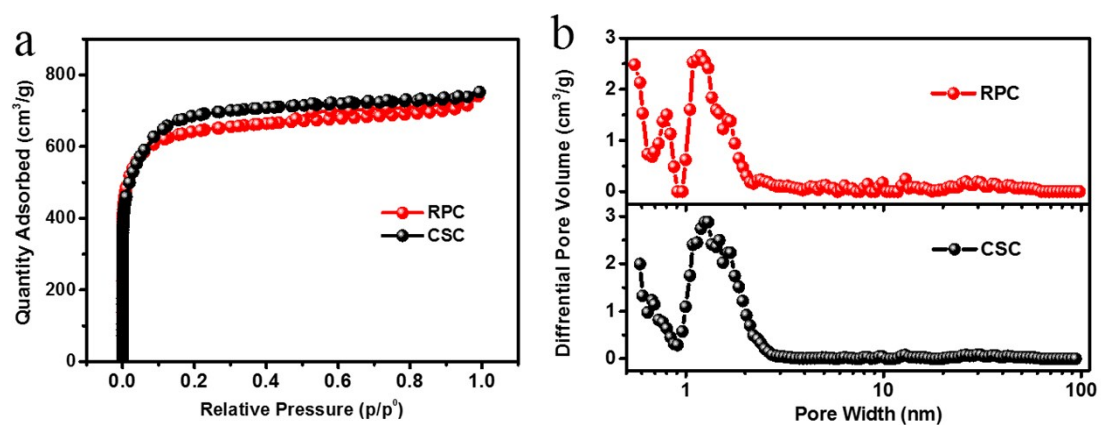


Figure S3. (a) N₂ adsorption-desorption curves of CSC and RPC. (b) pore-size distribution (PSD) curves of CSC and RPC.

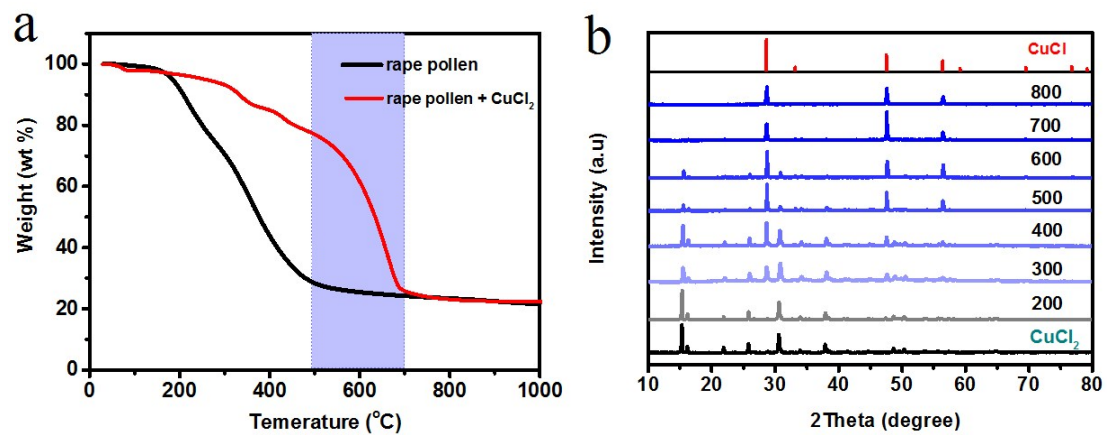
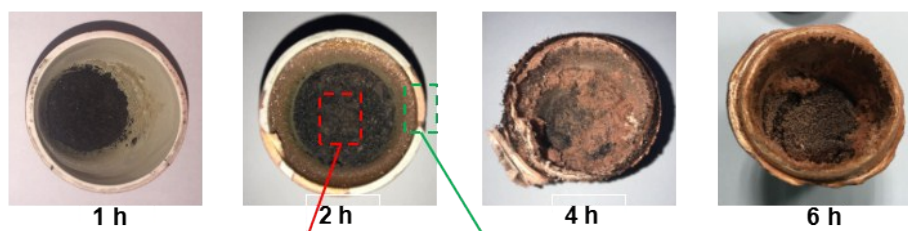
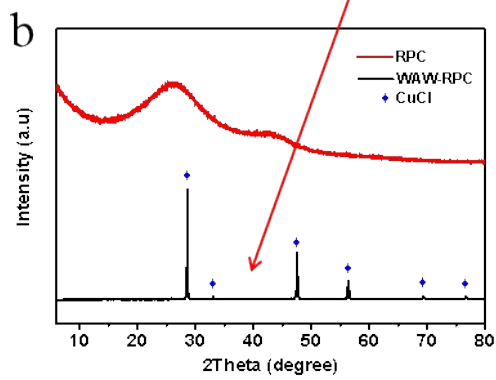


Figure S4. (a) The TGA curves of raw rape pollen and the mixture of rape pollen and CuCl₂ with weight ratio of 1:10 (rape pollen/ CuCl₂). (b) XRD patterns of the mixture of rape pollen and CuCl₂ with weight ratio of 1:10 (rape pollen/ CuCl₂) annealed at different temperatures (200 - 800 °C) in N₂ flow and without acid washing.

a



b



c

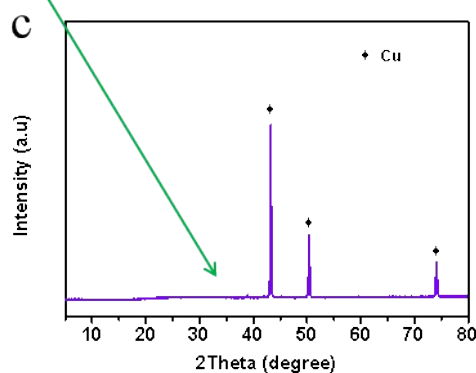


Figure S5. (a) image of WAW-RPC. (b) XRD patterns of WAW-RPC and RPC. (c) XRD patterns of the yellow product.

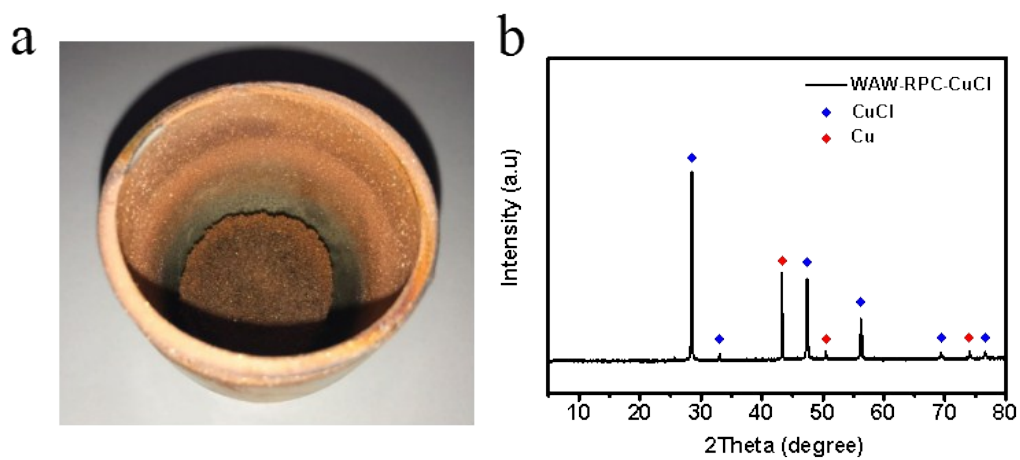


Figure S6. (a) image of WAW-RPC-CuCl. (b) XRD patterns of WAW-RPC-CuCl.

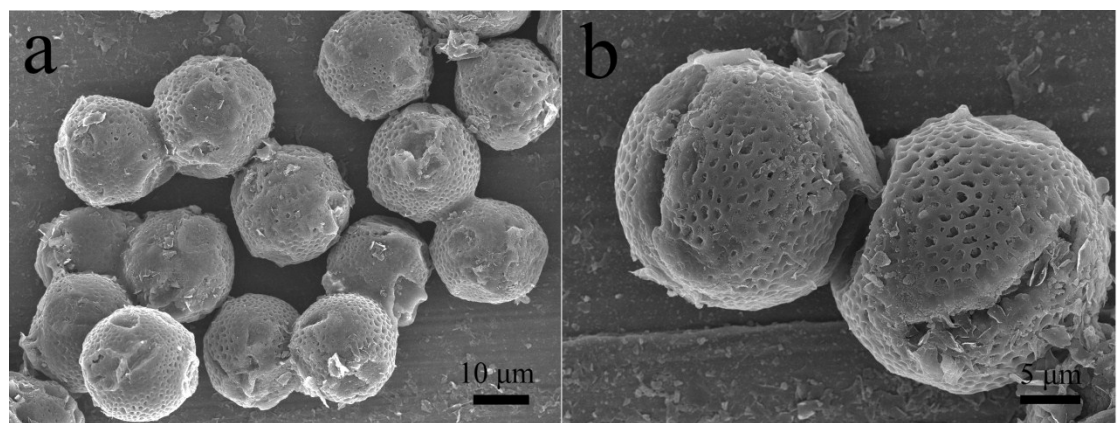


Figure S7. (a) SEM image of RPC-CuCl. (b) SEM image of RPC-CuCl at different magnification.

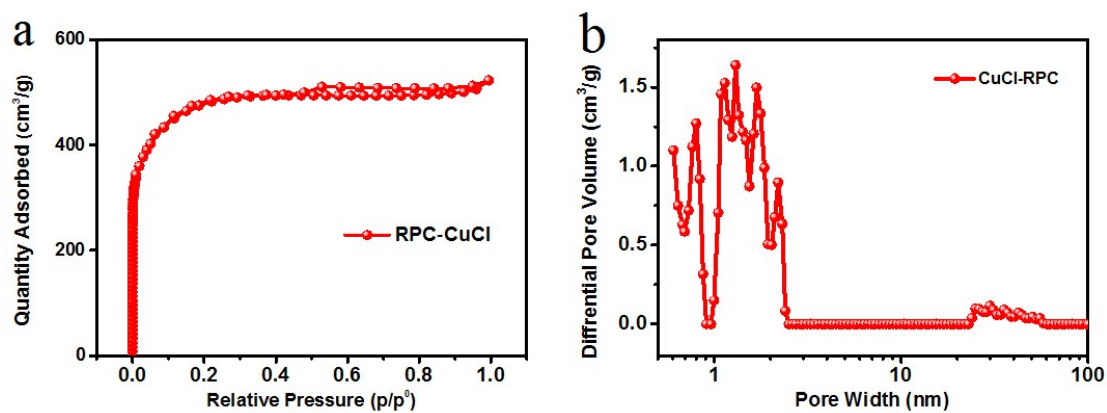


Figure S8. (a) N_2 adsorption-desorption curves of RPC-CuCl. (b) pore-size distribution (PSD) curves of RPC-CuCl.

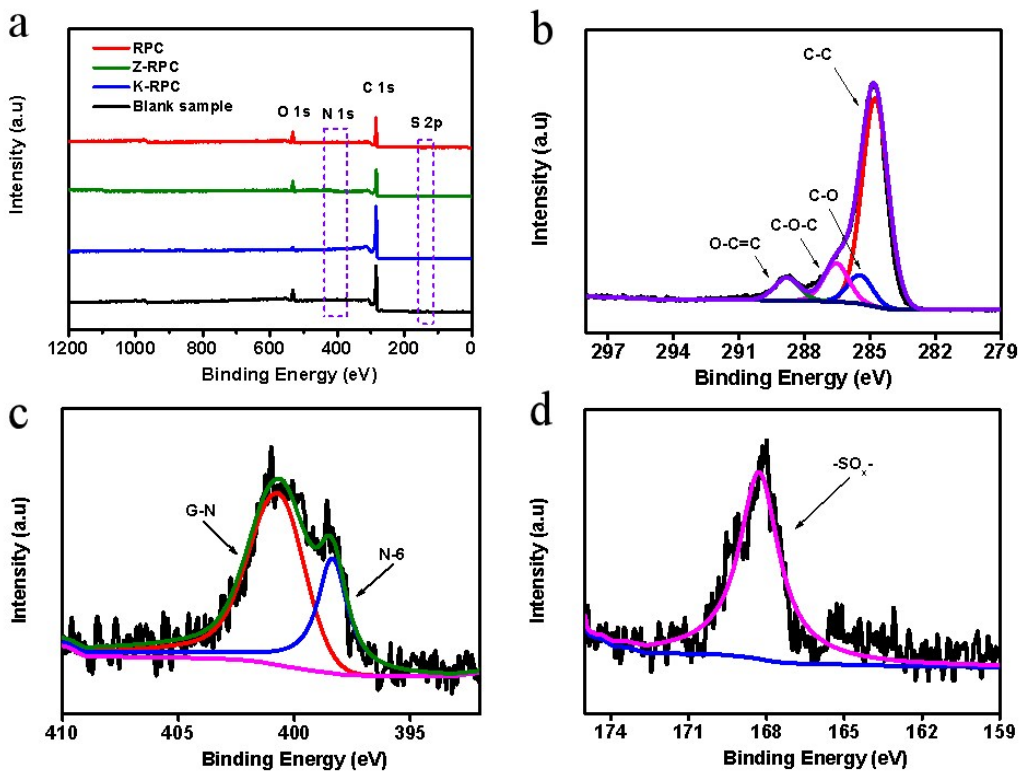


Figure S9. (a) XPS spectra of the samples. (b) high-resolution C1s of RPC. (c) High-resolution N 1s of RPC. (d) high-resolution S2p of RPC.

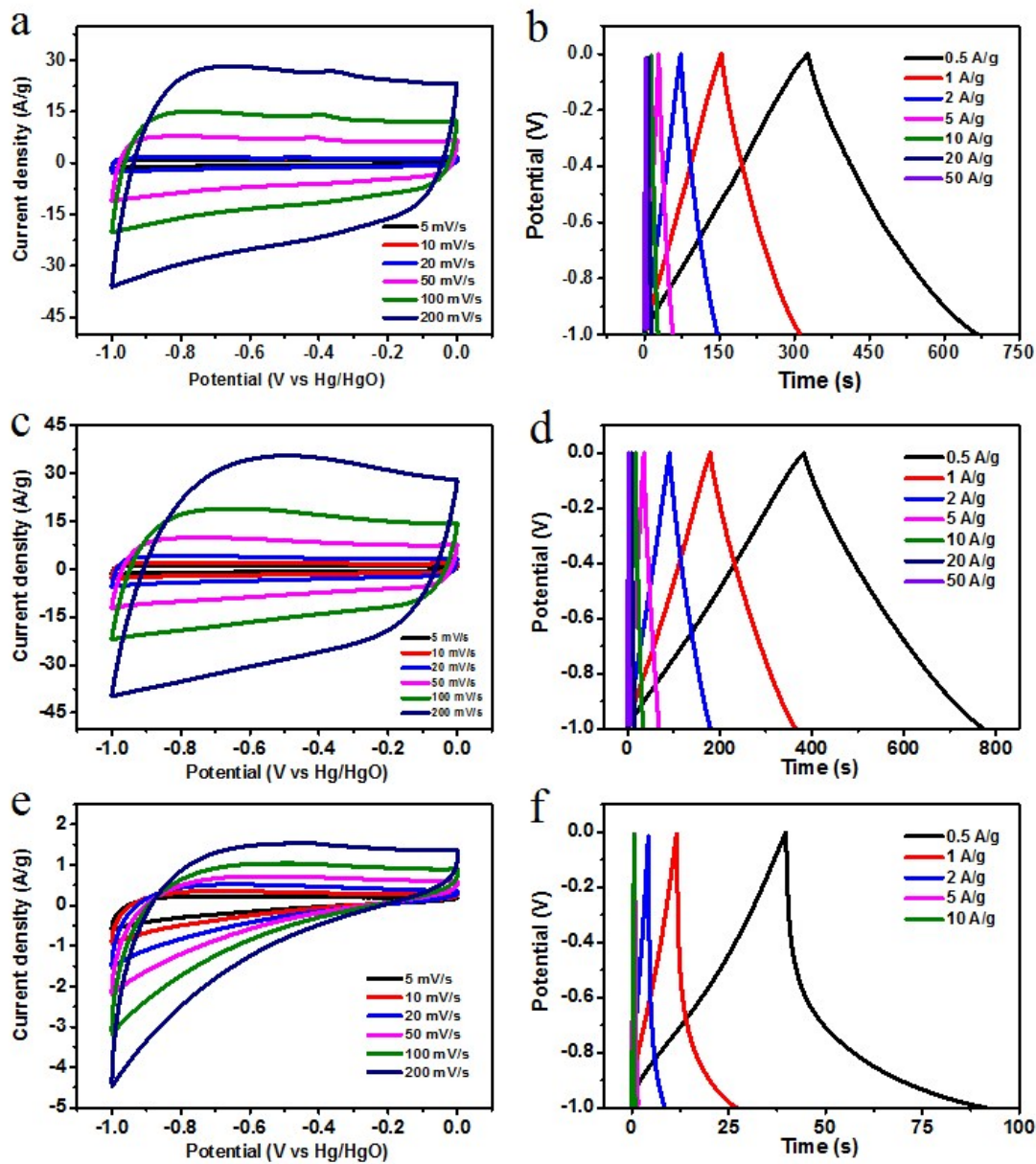


Figure S10. (a) CV curves of Z-RPC. (b) GCD curves of Z-RPC at different current density.(c) CV curves of K-RPC. (d) GCD curves of K-RPC at different current density. (e) CV curves of Blank sample. (f) GCD curves of Blank sample at different current density.

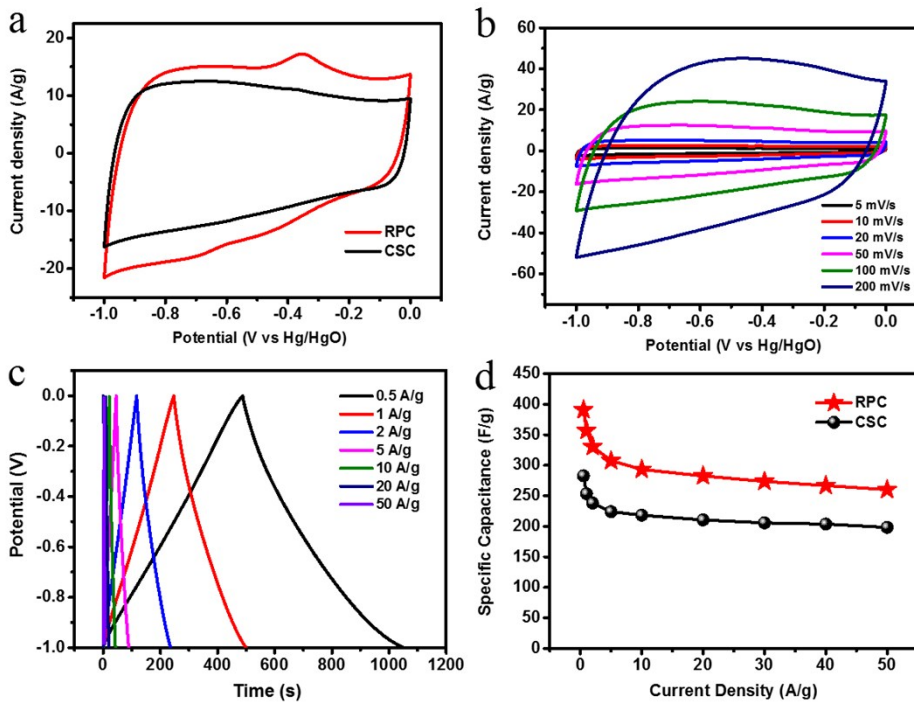


Figure S11. (a) CV curves of CSC and RPC at scan rate of 50 mV s^{-1} . (b) CV curves of CSC at different scan rate. (c) GCD curves of CSC at different current density. (d) Specific capacitance of CSC and RPC at different current density.

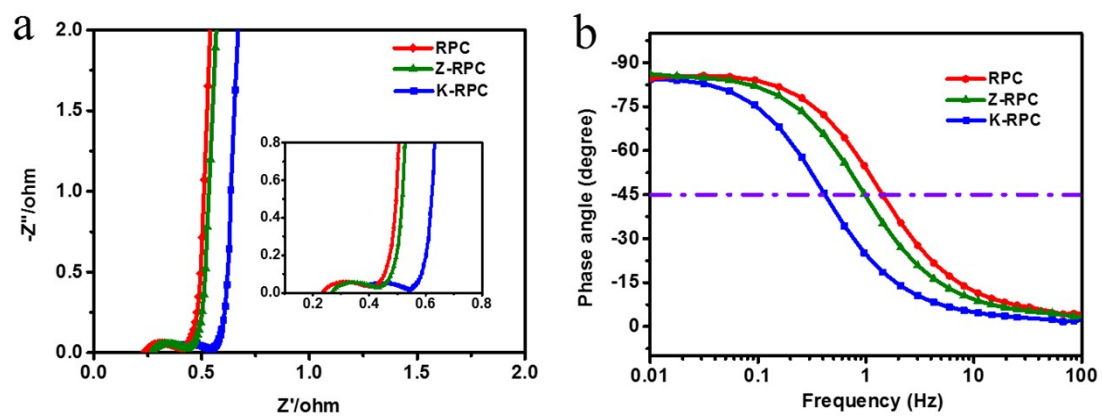


Figure S12. (a) Nyquist plots of RPC, Z-RPC and K-RPC. (b) Bode plots of RPC, Z-RPC and K-RPC.

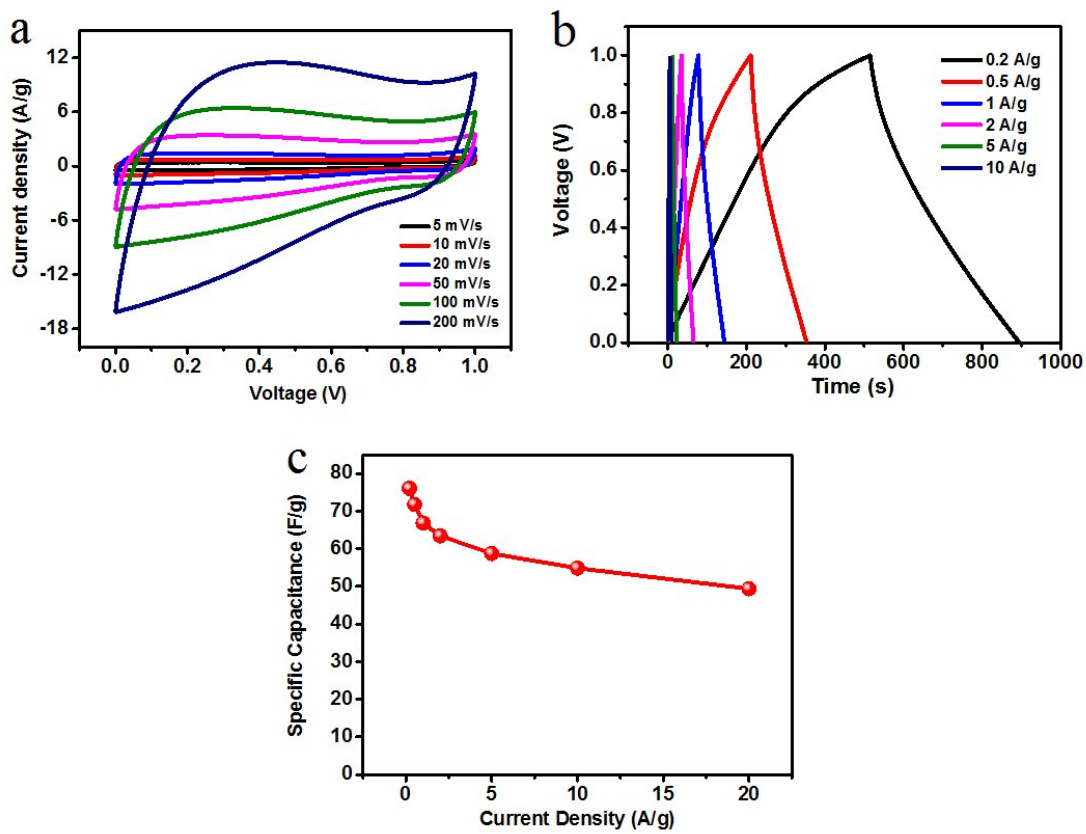


Figure S13. (a) CV curves of RPC at a different scan rate in two electrode system using 6.0 M KOH solution. (b) GCD curves of RPC at different current density in two electrode system using 6.0 M KOH solution. (c) Specific capacitances of RPC at different current densities in two electrode system using 6.0 M KOH solution.

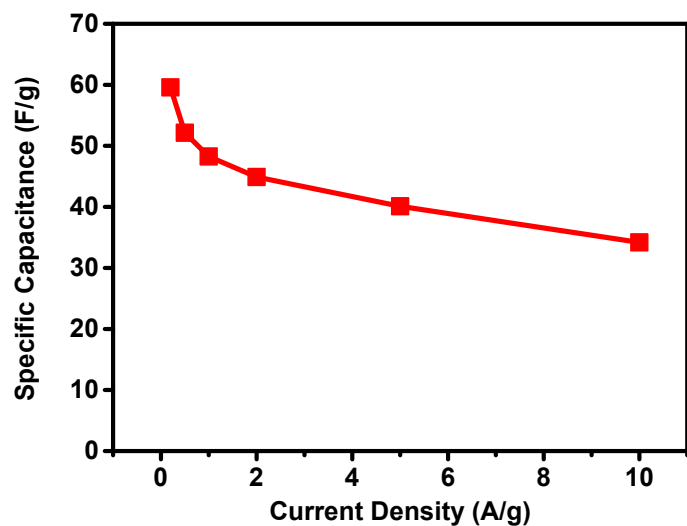


Figure S14. Specific capacitances of RPC at different current densities in two electrode system using 1.0 M Na_2SO_4 solution.

Table S1. The preparation condition of the samples.

Sample	Raw biomass	Activation	Carbonization	Acid wash
		agent	(at 900 °C)	
RPC	rape pollen	CuCl ₂	√	√
Z-RPC	rape pollen	ZnCl ₂	√	√
K-RPC	rape pollen	KOH	√	√
Blank sample	rape pollen	×	√	√
WAW-RPC	rape pollen	CuCl ₂	√	×
WAW-RPC-CuCl	rape pollen	CuCl	√	×
RPC-CuCl	rape pollen	CuCl	√	√
CSC	coconut shell	CuCl ₂	√	√

The √ represents the sample have treated with the condition, the × is the opposite.

Table S2. Porosity parameters and electrochemical performances of the as-prepared samples.

Samples	Yield ^[a]	S _{BET} ^(b)	S _{micro} ^(c)	S _{micro} /S _{BET} ^(d)	V _t ^(e)	V _{micro} ^(f)	D _{HK} ^(g)	D _{BJH} ^(h)	Gravimetric Capacitance (F g ⁻¹) ⁽ⁱ⁾
	(%)	[m ² g ⁻¹]	[m ² g ⁻¹]		[cm ³ g ⁻¹]	[cm ³ g ⁻¹]	[nm]	[nm]	
RPC	37.6	2488	2120	0.85	1.14	0.83	0.81	2.65	390
Z-RPC	28.3	1012	541	0.53	1.04	0.24	0.87	4.99	170
K-RPC	1.4	2016	1466	0.72	1.09	0.63	0.85	2.81	195
Blank sample	24.4	2.2	0	0	-	-	-	-	27
RPC-CuCl	35.2	1783	1256	0.70	0.81	0.49	0.80	2.2	-
CSC	19.9	2651	2217	0.83	1.16	0.86	0.86	2.6	283

- (a) The yield of the activated carbon.
- (b) Specific surface area from multiple BET (Brunauer–Emmett–Teller) method.
- (c) Micropore surface area from t-plot method.
- (d) The ratio of micropores specific surface area.
- (e) Total pore volume at P/P₀= 0.99.
- (f) The volume of micropores was determined by t-plot method.
- (g) D_{HK} represents the median micropore size by the Horvath-Kawazoe (HK) method.
- (h) D_{BJH} stands for the Barrett-Joyner-Halenda (BJH) desorption average pore width.
- (i) At a current density of 0.5 A g⁻¹.

Table S3 Comparison of CuCl₂ activation with the previously reported activating methods.

Activation agent	Raw materials	S _{BET} (m ² g ⁻¹)	Gravimetric Capacitance (F g ⁻¹)	Measurement Condition	Ref.
KOH	Lignin	2218	312	6 M KOH 1 A g ⁻¹	S1
KOH	Cellulose	2457	236	1M TEABF ₄ /AN 1 mV s ⁻¹	S2
KOH	Starch	1510	194	30 wt.% KOH 1 A g ⁻¹	S3
KOH	Coconut shell	1356	-	-	S4
KOH	Rape pollen	2756	176	Neat EMIMBF ₄ 1 A g ⁻¹	S5
KOH	Moringa oleifera branch	2312	355	6 M KOH 0.5 A g ⁻¹	S6
KOH	Willow Catkins	1775	292	6 M KOH 1 A g ⁻¹	S7
KOH	Chitosan	2435	291	6 M KOH 0.2 A g ⁻¹	S8
KOH	Pumpkin	2968	419	6 M KOH 0.5 A g ⁻¹	S9
KOH	sunflower seed shell	2585	311	6 M KOH 0.25 A g ⁻¹	S10
KOH	Wheat straw	2316	251	MeEt ₃ NBF ₄ /AN 2 mV s ⁻¹	S11
K ₂ CO ₃	Chitosan	1013	246	3 M KOH 0.5 A g ⁻¹	S12
K ₂ CO ₃	Reed Black Liquor	1395	-	-	S13
K ₂ CO ₃	Glucose	2150	-	-	S14
KHCO ₃	Glucose	2230	246	1 M H ₂ SO ₄ 0.1 A g ⁻¹	S14
NaOH	Rice husk	1886	214	3 M KCl -	S15
Na ₂ CO ₃	Chitosan	440	-	-	S16
NaHCO ₃	Bluestem	552	220	6 M KOH 0.1 A g ⁻¹	S17

ZnCl ₂	Chitosan	1582	252	6 M KOH 0.5 A g ⁻¹	S18
ZnCl ₂	Coconut shell	1266	-	-	S19
ZnCl ₂	Spider silk	721	-	-	S20
ZnCl ₂ +FeCl ₃	Moringa oleifera stems	2250	283	6 M KOH 0.5 A g ⁻¹	S21
ZnCl ₂ +FeCl ₃	Silk	2494	242	EMIMBF4 0.1 A g ⁻¹	S22
ZnCl ₂ +FeCl ₃	Coconut shell	1874	268	6 M KOH 1 A g ⁻¹	S23
ZnCl ₂ +KCl	Glucose	2160	206	6 M KOH 5 mV s ⁻¹	S24
CO ₂	Coconut shell	1667	-	-	S25
CO ₂	Chitosan	1054	194	1 M H ₂ SO ₄ 0.2 A g ⁻¹	S26
NH ₃	Typha orientalis	898	-	-	S27
NH ₃	Cellulose	1326	-	-	S28
Steam	Coconut shell	1559	228	6 M KOH 5 mV s ⁻¹	S29
Steam	Wood	1131	142	0.5 M H ₂ SO ₄ 3 mA cm ²	S30
KOH+CO ₂	Coconut shell	1026	-	-	S31
K ₂ FeO ₄	Bamboo	1732	222	6 M KOH 0.5 A g ⁻¹	S32
CuCl ₂	Rape pollen	2488	390	6 M KOH 0.5 A g ⁻¹	This work

Table S4. Contents of C1s, O1s, N1s and S2p of the as-resulted samples.

Samples	XPS (atom %)				Element analysis (wt %)			
	C	O	N	S	C	O	N	S
RPC	81.4	13.6	4.0	0.5	65.8	25.1	4.0	1.1
Z-RPC	83.2	12.9	3.0	0.4	78.3	15.2	3.2	1.0
K-RPC	91.1	8.7	0	0	89.1	6.4	0.1	0.5
Blank sample	94.4	3.57	1.67	0.33	71.0	23.9	3.7	0.3
CSC	85.05	14.79	0	0	71.4	26.8	0	0

References.

1. L. Zhang, T. You, T. Zhou, X. Zhou and F. Xu, *ACS applied materials & interfaces*, 2016, **8**, 13918-13925.
2. L. Wei, M. Sevilla, A. B. Fuertes, R. Mokaya and G. Yushin, *Advanced Energy Materials*, 2011, **1**, 356-361.
3. Q. Li, H. Wang, Q. Dai, J. Yang and Y. Zhong, *Solid State Ionics*, 2008, **179**, 269-273.
4. K. Y. Foo and B. H. Hameed, *Chemical Engineering Journal*, 2012, **184**, 57-65.
5. L. Zhang, F. Zhang, X. Yang, K. Leng, Y. Huang and Y. Chen, *Small*, 2013, **9**, 1342-1347.
6. Y. Cai, Y. Luo, Y. Xiao, X. Zhao, Y. Liang, H. Hu, H. Dong, L. Sun, Y. Liu and M. Zheng, *ACS applied materials & interfaces*, 2016, **8**, 33060-33071.
7. L. Xie, G. Sun, F. Su, X. Guo, Q. Kong, X. Li, X. Huang, L. Wan, K. Li and C. Lv, *Journal of Materials Chemistry A*, 2016, **4**, 1637-1646.
8. P. Hao, Z. Zhao, Y. Leng, J. Tian, Y. Sang, R. I. Boughton, C. P. Wong, H. Liu and B. Yang, *Nano Energy*, 2015, **15**, 9-23.
9. G. Sun, B. Li, J. Ran, X. Shen and H. Tong, *Electrochimica Acta*, 2015, **171**, 13-22.

10. X. Li, W. Xing, S. Zhuo, J. Zhou, F. Li, S. Z. Qiao and G. Q. Lu, *Bioresour Technol*, 2011, **102**, 1118-1123.
11. X. Li, C. Han, X. Chen and C. Shi, *Microporous and Mesoporous Materials*, 2010, **131**, 303-309.
12. F. Zhang, T. Liu, G. Hou, T. Kou, L. Yue, R. Guan and Y. Li, *Nano Research*, 2016, **9**, 2875-2888.
13. Y. Sun, J. P. Zhang, G. Yang and Z. H. Li, *Environ Technol*, 2007, **28**, 491-497.
14. M. Sevilla and A. B. Fuertes, *ChemSusChem*, 2016, **9**, 1880-1888.
15. Y. Guo, J. Qi, Y. Jiang, S. Yang, Z. Wang and H. Xu, *Materials Chemistry and Physics*, 2003, **80**, 704-709.
16. A. Kucinska, A. Cyganiuk and J. P. Lukaszewicz, *Carbon*, 2012, **50**, 3098-3101.
17. H. Jin, X. Wang, Z. Gu, J. D. Hoefelmeyer, K. Muthukumarappan and J. Julson, *RSC Advances*, 2014, **4**.
18. X. Deng, B. Zhao, L. Zhu and Z. Shao, *Carbon*, 2015, **93**, 48-58.
19. D. C. S. Azevedo, J. C. S. Araújo, M. Bastos-Neto, A. E. B. Torres, E. F. Jaguaribe and C. L. Cavalcante, *Microporous and Mesoporous Materials*, 2007, **100**, 361-364.
20. L. Zhou, P. Fu, X. Cai, S. Zhou and Y. Yuan, *Applied Catalysis B: Environmental*, 2016, **188**, 31-38.
21. Y. Cai, Y. Luo, H. Dong, X. Zhao, Y. Xiao, Y. Liang, H. Hu, Y. Liu and M. Zheng, *Journal of Power Sources*, 2017, **353**, 260-269.
22. J. Hou, C. Cao, F. Idrees and X. Ma, *ACS nano*, 2015, **9**, 2556-2564.
23. L. Sun, C. Tian, M. Li, X. Meng, L. Wang, R. Wang, J. Yin and H. Fu, *Journal of Materials Chemistry A*, 2013, **1**, 6462.
24. J. Pampel, C. Denton and T.-P. Fellinger, *Carbon*, 2016, **107**, 288-296.
25. K. Yang, J. Peng, H. Xia, L. Zhang, C. Srinivasakannan and S. Guo, *Journal of the Taiwan Institute of Chemical Engineers*, 2010, **41**, 367-372.
26. A. Śliwak, N. Díez, E. Miniach and G. Gryglewicz, *Journal of Applied Electrochemistry*, 2016, **46**, 667-677.
27. P. Chen, L.-K. Wang, G. Wang, M.-R. Gao, J. Ge, W.-J. Yuan, Y.-H. Shen, A.-J. Xie and S.-H. Yu, *Energy Environ. Sci.*, 2014, **7**, 4095-4103.
28. W. Luo, B. Wang, C. G. Heron, M. J. Allen, J. Morre, C. S. Maier, W. F. Stickle and X. Ji, *Nano Lett*, 2014, **14**, 2225-2229.
29. J. Mi, X.-R. Wang, R.-J. Fan, W.-H. Qu and W.-C. Li, *Energy & Fuels*, 2012, **26**, 5321-5329.
30. F.-C. Wu, R.-L. Tseng, C.-C. Hu and C.-C. Wang, *Journal of Power Sources*, 2006, **159**, 1532-1542.
31. A. T. Mohd Din, B. H. Hameed and A. L. Ahmad, *J Hazard Mater*, 2009, **161**, 1522-1529.
32. Y. Gong, D. Li, C. Luo, Q. Fu and C. Pan, *Green Chemistry*, 2017, **19**, 4132-4140.